https://dx.doi.org/10.4314/dujopas.v10i3a.28
ISSN (Print): 2476-8316
ISSN (Online): 2635-3490
Dutse Journal of Pure and Applied Sciences (DUJOPAS), *Vol. 10 No. 3a September 2024*

Unraveling the Influence of Oxygen Vacancy with and Without Replacement on Cu_2O: A DFT Study

Ibrahim Ismail Idowu[1], Lawal Mohammed[2], Sadiq Umar[2], Adamu Uzairu[4], Bashir Yusuf[2], Yahaya Saadu Itas[3]

[1] Department of Physics,
Federal University Dutse,
Dutse 720101,
Nigeria.

[2] Department of Physics,
Ahmadu Bello University Zaria
810282, Kaduna,
Nigeria.

[3]Department of Physics,
Bauchi State University Gadau,
PMB 65, Gadau 751105,
Nigeria.

[4]Department of Chemistry
Ahmadu Bello University Zaria
810282, Kaduna,
Nigeria.

Abstract

This study delves into the structural and electronic effects of oxygen vacancies in Cu_2O using density functional theory (DFT) enhanced with Hubbard U corrections (DFT+U). A 3x2x1 supercell of Cu_2O was employed. The study meticulously investigates the removal of 1, 2, and 3 oxygen atoms, analyzing the ensuing changes in both structural stability and electronic properties, with particular emphasis on the band gap.The structural analysis revealed that oxygen vacancy formation induces significant modifications in Cu-O and Cu-Cu bond lengths, with elongations observed around the vacancy sites in which the Cu-Cu bond length decreased to 2.4035 Å, compared to 3.0066 Å in the pristine structure. The structural distortion followed the Jahn-Teller effect, leading to the formation of isolated units and transformation in bond angles. The introduction of oxygen vacancies without replacement (WOR) caused significant distortions in the Cu_2O lattice, which were more pronounced with increasing vacancy concentration. The Cu-O bond length increased from 1.8492 Å in the pristine structure to 1.9840 Å in the single vacancy configuration. However, in the oxygen vacancies with replacement (WR) the Cu-Cu bond length increased slightly to 3.0218 Å, with the Cu-O bond length expanding to 1.8505 Å. The band structure analysis indicated a decrease in the band gap with increasing vacancy concentration. The pristine Cu_2O exhibited a band gap of 1.67 eV as calculated, which was increased to 1.97 eV with a single vacancy and 1.16 eV with two vacancies, reflecting the significant impact of oxygen vacancies on the material's optoelectronic properties. The findings underscore the critical role of oxygen vacancies in modulating the structural and electronic properties of Cu_2O, providing insights that are pivotal for optimizing its performance in applications like photocatalysis and solar cells.

Keywords: Cu_2O, DFT+U, Hubbard Value, Oxygen Vacancies, Jahn Teller effect.

Author for Correspondence

INTRODUCTION

Cuprous oxide (Cu_2O) is a p-type semiconductor with a direct band gap of approximately 2.1 eV, making it a promising candidate for various applications, including photocatalysis, solar cells, and gas sensors (Hu et al., 2008). The material's electronic and optical properties can be significantly influenced by intrinsic defects, particularly oxygen vacancies, which are known to act as shallow donors and modify the material's electrical conductivity and optical absorption. These vacancies can alter the electronic structure, potentially improving or degrading the performance of Cu_2O in its intended applications.

Previous studies have demonstrated that oxygen vacancies play a crucial role in modifying the band gap, carrier concentration, and overall stability of Cu_2O (Dongfang et al., 2023). Li et al. (2018) used density functional theory (DFT) to explore how oxygen vacancies affect the electronic structure of Cu_2O. They discovered that an increase in vacancy concentration leads to a significant reduction in the band gap, indicating that Cu_2O's optoelectronic properties are highly sensitive to oxygen vacancies. In a different study, Zhuang et al. (2020) focused on the catalytic properties of Cu_2O with oxygen vacancies. Their research showed that the presence of these vacancies enhances catalytic activity due to changes in the electronic configuration, suggesting that Cu_2O with vacancies has potential as a catalyst in various applications.

However, a comprehensive understanding of the impact of different oxygen vacancy concentrations and configurations on the structural and electronic properties remains limited. To address this, we employ density functional theory (DFT) with Hubbard U corrections (DFT+U) to systematically investigate the effects of oxygen vacancies on Cu_2O.

In this study, we explore the formation of oxygen vacancies in Cu_2O using a 3x2x1 supercell (Figure 1b) and assess how varying vacancy concentrations influence bond lengths, structural distortions, and the electronic band structure. By comparing oxygen vacancies with and without replacement atoms, we aim to provide insights into the mechanisms driving the observed changes, contributing to the optimization of Cu_2O for advanced technological applications.

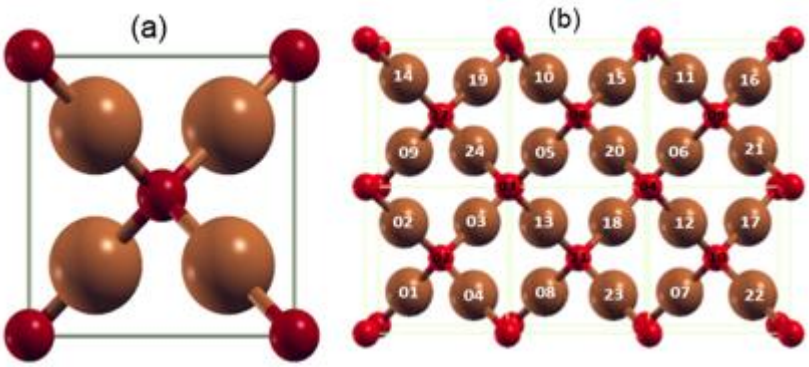

Figure 1: Depicts the structure of (a) unit cell of Cu_2O (b) 3x2x1 Supercell indicating its atomic positions. The brown and red spheres represent Cu and O atom respectively.

METHODOLOGY

The investigation employs a 3x2x1 supercell of Cu_2O, consisting of 24 Cu atoms and 12 O atoms. Quantum ESPRESSO (Giannozzi et al., 2009), an open source DFT code, is used for the simulations, with ultrasoft pseudopotentials to accurately capture electron-ion interactions. The study incorporates the removal of 1 to 6 oxygen atoms, emphasizing the first three at atomic positions O33, O32, and O35. The simulations use the Monkhorst–Pack scheme (Wang et al., 2021) for k-point sampling with a grid density of 8x8x8, and an energy cut-off of 45 Ry.

To refine the structural geometry, the Broyden–Fletcher–Goldfarb–Shanno (BFGS) method is applied, with force and energy convergence criteria set to 0.002 eV and 10^{-4} eV, respectively. Given the limitations of the Generalized Gradient Approximation (GGA) (Perdew et al., 1996) in predicting band gaps, the DFT+U(Cadi-Essadek et al., 2021; Kirchner-Hall et al., 2021) formalism is employed, introducing Hubbard-U terms of 8.5 eV for Cu-3d and O-2p orbitals. The U value applied to O 2p is to account for the change in the electronic structure due to the induced states caused by the vacancy. This approach aims to enhance the accuracy of the band gap calculations.

RESULTS AND DISCUSSION

Optimized Structural Properties of the Pristine Cu_2O

The study first examines the relaxed structural properties of pristine Cu_2O. The calculated lattice constant of 4.2696 Å and bond lengths such as Cu-Cu (3.0066 Å) and Cu-O (1.8412 Å) closely match previous work of (Li et al., 2011), confirming the reliability of the model. The angles formed by O − Cu − O (within the cavity and the O rings) was measured to be 109.471°, confirming the tetrahedral bond angle of the structure.

Similarly, the relaxed structure of the 3x2x1 pure cuprous oxide supercell ($Cu_{24}O_{12}$), consists of 6 units of Cu_2O with a total of 24 Cu and 12 O atoms. The averaged lattice parameters of the Cu – O bond length linking the Cu_2O unit and the lattice constant in the pure 3x2x1 $Cu_{24}O_{12}$ were found to be 3.5232 Å and 8.5040 Å respectively.

Table 1: Showing the calculated bond length and formation energy of Pristine Cu_2O

Type of calculation	BEFORE RELAXATION					AFTER RELAXATION			Bandgap (eV)	Formation Energy (eV)
	Atomic ID	Cu-Cu (A^0)	Cu-O (A^0)	O-O (A^0)	Atomic ID	Cu-Cu (A^0)	Cu-O (A^0)	O-O (A^0)		
Pristine Cu_2O	Cu6-Cu16	3.0198			Cu6-Cu16	3.0218				
	Cu15-O33		1.8492		Cu15-O33		1.8505		1.67	-9.16552072
	O27-O33			3.6985	O27-O33			3.6985		

The structural parameters obtained in our study align consistently with established references (Bogenrieder et al., 2024). The before-relaxation nearest neighbor (NN) Cu-Cu distances measure 3.0198 Å, while the Cu-O and O-O distances are 1.8492 Å and 3.6985 Å, respectively.

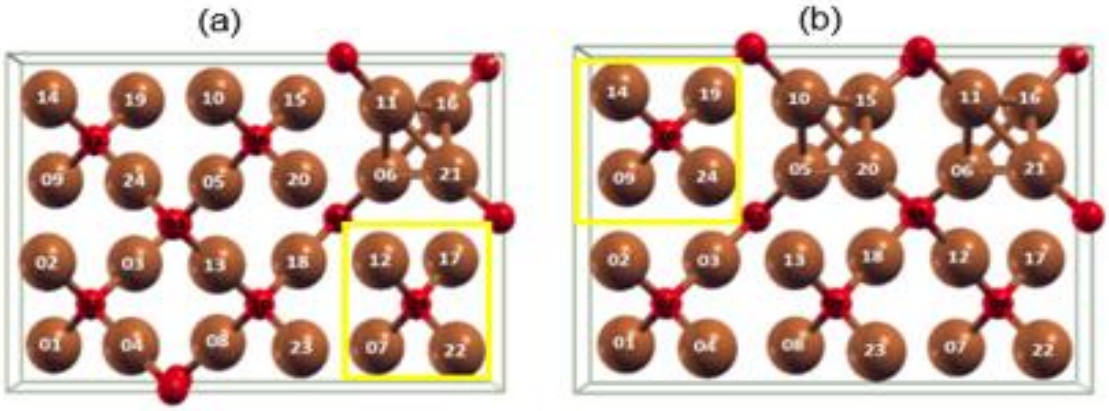

Figure 2: Shows the structural transformation effect of one, and two oxygen vacancy after relaxation respectively.

However, after relaxation it was observed that the system undergoes several strains that invoke the bond between the vacant site and reconnecting same between the Cu-Cu atoms forming a diamond or pyramid like structure as shown in Figure 2. The bond distances formed around the regular octahedral network structure for the one vacancy shows that Cu6-Cu16 is equal in length with Cu11-Cu21 with same bond length of 2.4035(Å), also Cu11-Cu6 and Cu16-Cu21 has the same bond distance of 2.7055(Å), while that of Cu11-Cu16 and Cu6-Cu21 has a bond distance of 2.6321(Å) this is closely related to what was obtained by (Dongfang et al., 2023).

Also, for the two vacancies, it was observed that Cu11-Cu21 is equal in length with Cu16-Cu6 with same bond length of 2.4375(Å), while Cu11-Cu6, Cu11-Cu16, Cu16-Cu21 and Cu21-Cu6 have different bond lengths of 2.7382(Å), 2.7259(Å), 2.7728(Å) and 2.6905(Å) (Dongfang et al., 2023) respectively. The modulation behavior is as represented in the histogram shown in figure 3(a), and (b).

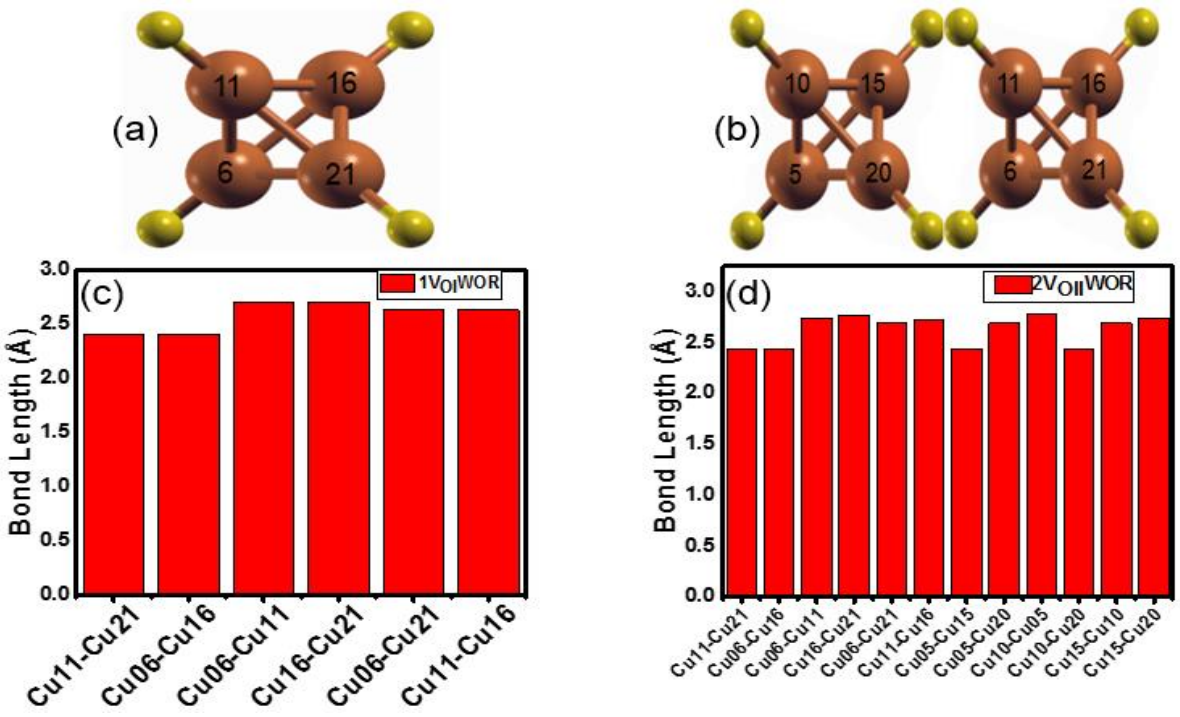

Figure 3: Depicts (a) one vacancy after relaxation bond distances (b) two vacancies after relaxation bond distances (c) the histogram representation of bond length with one vacancy (d) the histogram representation of bond length with two vacancies.

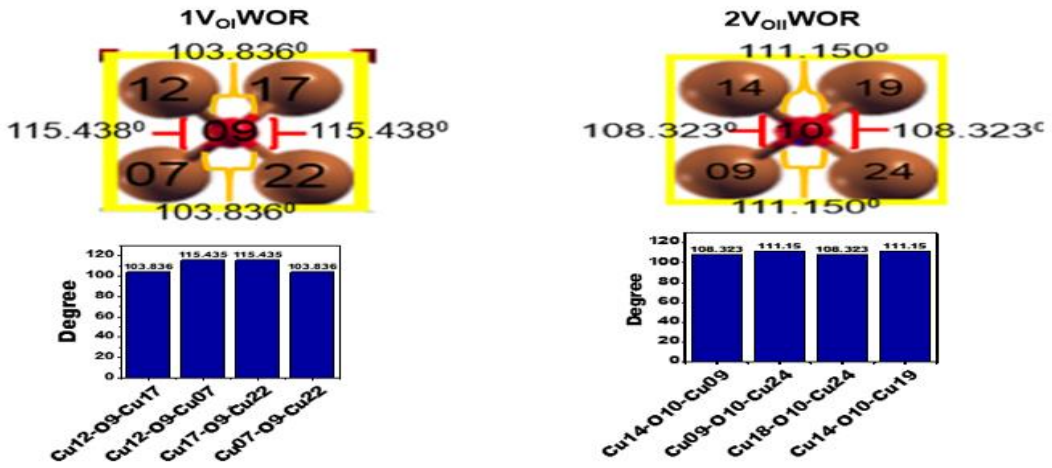

Figure 4: Variation of bond angles for the first and second oxygen vacancy WOR with the histogram showing the modulation effect.

Electronic Effect of Oxygen Vacancy Without Replacement. (WOR)

When an oxygen atom is removed without replacement (WOR), the nearest Cu atoms around the vacancy experience varying degrees of bond elongation (Figure 5), indicative of a Jahn-Teller distortion. This structural alteration leads to changes in bond lengths and angles, which are reflected in the electronic structure of the material. For example, bond lengths such as Cu6-Cu16 and Cu11-Cu21 in the one-vacancy system equalize at 2.4035 Å after relaxation, while in the two-vacancy system, distinct bond lengths emerge, suggesting a more complex distortion pattern.

Structural transformations due to vacancy formation are significant, with strains leading to the disconnection of the Cu-O-Cu interatomic network. This distortion, driven by bond elongation and compression, results in isolated monomer cells, impacting the electronic and optical properties of Cu_2O. The observed Jahn-Teller distortion (Tarantino et al., 2016) effects are crucial in understanding the vacancy-induced modulation of the electronic structure.

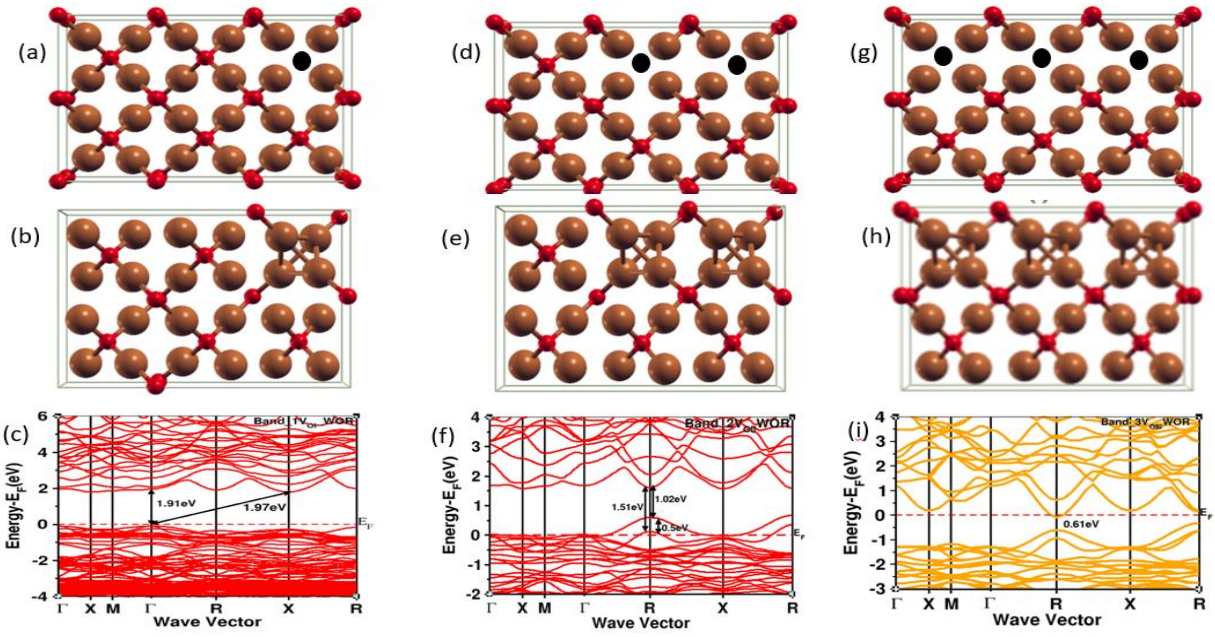

Figure 5. Structure (a,d, and g) is before relaxation and (b,e and h) is after relaxation for Cu_2O. (a, b and c) before and after relaxation with electronic band structure for one oxygen vacancy; (d, e and f) before and after relaxation, with electronic band structure for two oxygen vacancy (g,h, and i) before and after relaxation, with electronic band structure for three oxygen vacancy. The brown, and red spheres represent Cu and O atom respectively while the black sphere represent the vacant sites.

From the result in Figure 5, it was observed that the structure before relaxation (Figure 5a), the vacancy is well-defined. After relaxation (Figure 5b), the surrounding atoms shift to accommodate the missing oxygen, leading to slight structural distortions. The band Structure (Figure 5c), exhibit both indirect and direct bandgap around 1.91 eV to 1.97 eV respectively, which fairly correspond with (Visibile et al., 2019). This indicates that the creation of a single oxygen vacancy introduces localized defect states within the bandgap, but it does not drastically alter the overall electronic structure. The presence of these defect states contributes to the conductivity by providing additional electrons to the conduction band compare with the pristine electronic structure.

For the two oxygen vacancies the structure (Figure 5d) before relaxation shows more significant disruption. After relaxation (figure 5e), the lattice undergoes more considerable distortion to compensate for the missing oxygen atoms mimicking the Jahn teller effect to maintain its stability.

The bandgap decreases to around 1.15eV with a double dispersion peak, a similar behavior was reported earlier for Cu_2O by inducing compressing strain on the unit cell up to ±10% (Visibile et al., 2019). This reduction is more pronounced, indicating that the additional vacancy states introduced are closer to the conduction band, further narrowing the bandgap. This suggests increased in conductivity due to a higher density of states near the conduction band, allowing more electrons to be thermally excited at a given temperature.

At the three oxygen vacancies the structure before relaxation (Figure 5g), is highly disrupted by the three vacancies. After relaxation (Figure 5h), the lattice attempts to stabilize, leading to significant atomic displacements. The bandgap further reduces to around 0.61 eV. This substantial reduction indicates that the material is approaching a narrow-gap semiconductor or even semi -metallic behavior. The defect states introduced by the three vacancies are likely merging with the conduction band, increasing the overlap between the valence and conduction bands. This could lead to a high density of free electrons and thus much higher conductivity.

The trend in the bandgap decreases progressively as the number of oxygen vacancies increases. This trend reflects the increasing influence of defect states within the bandgap, which progressively narrow the energy gap. The presence of oxygen vacancies introduces donor states, which likely contribute to n-type conductivity. The narrowing bandgap suggests an increase in the number of free electrons as vacancies increase.

Therefore, the potential transition is that as more vacancies are introduced, the material may transit from a semiconductor with a moderate bandgap to a material with semi-metallic properties, especially if the trend of bandgap reduction continues with further vacancies, this leads to higher electron concentrations and potential shifts in the Fermi level closer to the conduction band, indicating enhanced n-type behavior. Table 2,3 and 4, below shows the measured bond length, for the first, second and third oxygen vacancy WOR calculations.

Table 2: Showing the calculated bond length and formation energy of One Oxygen Vacancy without Replacement. The color map shows the modulation of the bond length in line with the Jahn teller effect

Type of calculation	BEFORE RELAXATION				AFTER RELAXATION				Bandgap (eV)	Formation Energy (eV)
	Atomic ID	Cu-Cu (A^0)	Cu-O (A^0)	O-O (A^0)	Atomic ID	Cu-Cu (A^0)	Cu-O (A^0)	O-O (A^0)		
$1V_{01}$	Cu6-Cu11	3.0066			Cu6-Cu11	2.7055			1.97	-6.662765428
	Cu15-O33		1.8412		Cu16-Cu21	2.7055				
	O27-O33			3.6823	Cu6-Cu16	2.4035				
					Cu11-Cu21	2.4035				
					Cu11-Cu16	2.6321				
					Cu6-Cu21	2.6321				
					Cu6-O27		1.9775			
					Cu11-O33		1.9775			
					Cu16-O36		1.9840			
					Cu21-O35		1.9840			

Table 3: Showing the calculated bond length and formation energy of Two Oxygen Vacancy without Replacement.

Type of calculation	BEFORE RELAXATION				AFTER RELAXATION				Band Gap (eV)	Formation Energy (eV)
	Atomic ID	Cu-Cu (A^0)	Cu-O (A^0)	O-O (A^0)	Atomic ID	Cu-Cu (A^0)	Cu-O (A^0)	O-O (A^0)		
$2V_{0III}$	Cu6-Cu11	2.4375			Cu6-Cu11	2.8208			1.53	-4.326502448
	Cu6-O27		1.8786		Cu6-Cu16	2.4375				
	O27-O33			5.8182	Cu11-Cu21	2.4375				
					Cu16-Cu21	2.7728				
					Cu11-Cu16	2.7259				
					Cu6-Cu21	2.7259				
					Cu6-O27		1.9775			
					Cu11-O33		1.9775			
					Cu16-O36		1.9840			
					Cu21-O35		1.9840			

Table 4: Showing the calculated bond length and formation energy of Three Oxygen Vacancy without Replacement

Type of calculation	BEFORE RELAXATION				AFTER RELAXATION				Band Gap (eV)	Formation Energy (eV)
	Atomic ID	Cu-Cu (A^0)	Cu-O (A^0)	O-O (A^0)	Atomic ID	Cu-Cu (A^0)	Cu-O (A^0)	O-O (A^0)		
$3V_{OIII}$					Cu6-Cu11	2.8279			1.16	-1.996130092
					Cu6-Cu16	2.4673				
					Cu11-Cu21	2.4673				
					Cu16-Cu21	2.8279				
					Cu11-Cu16	2.7784				
					Cu6-Cu21	2.7784				
					Cu6-O27		1.8950			
					Cu11-O33		1.8950			
					Cu16-O36		1.9910			
					Cu21-O35		1.9910			
					O-O(NNN)			5.8588		
					O-O(NNN)			5.8588		
					O-O(NN)			3.7749		
					O-O(NN)			3.7749		

Electronic Effect of Oxygen Vacancy with Replacement (WR)

In the WR scenario, the removal and replacement process cause the system to undergo structural relaxation, leading to changes in bond lengths and angles that differ from the WOR case. For instance, the Cu-Cu bond length extends to 3.0218 Å after relaxation, while the Cu-O bond remains relatively stable. The lattice parameters indicate an expansion of the lattice, influenced by the vacancy-induced strain.

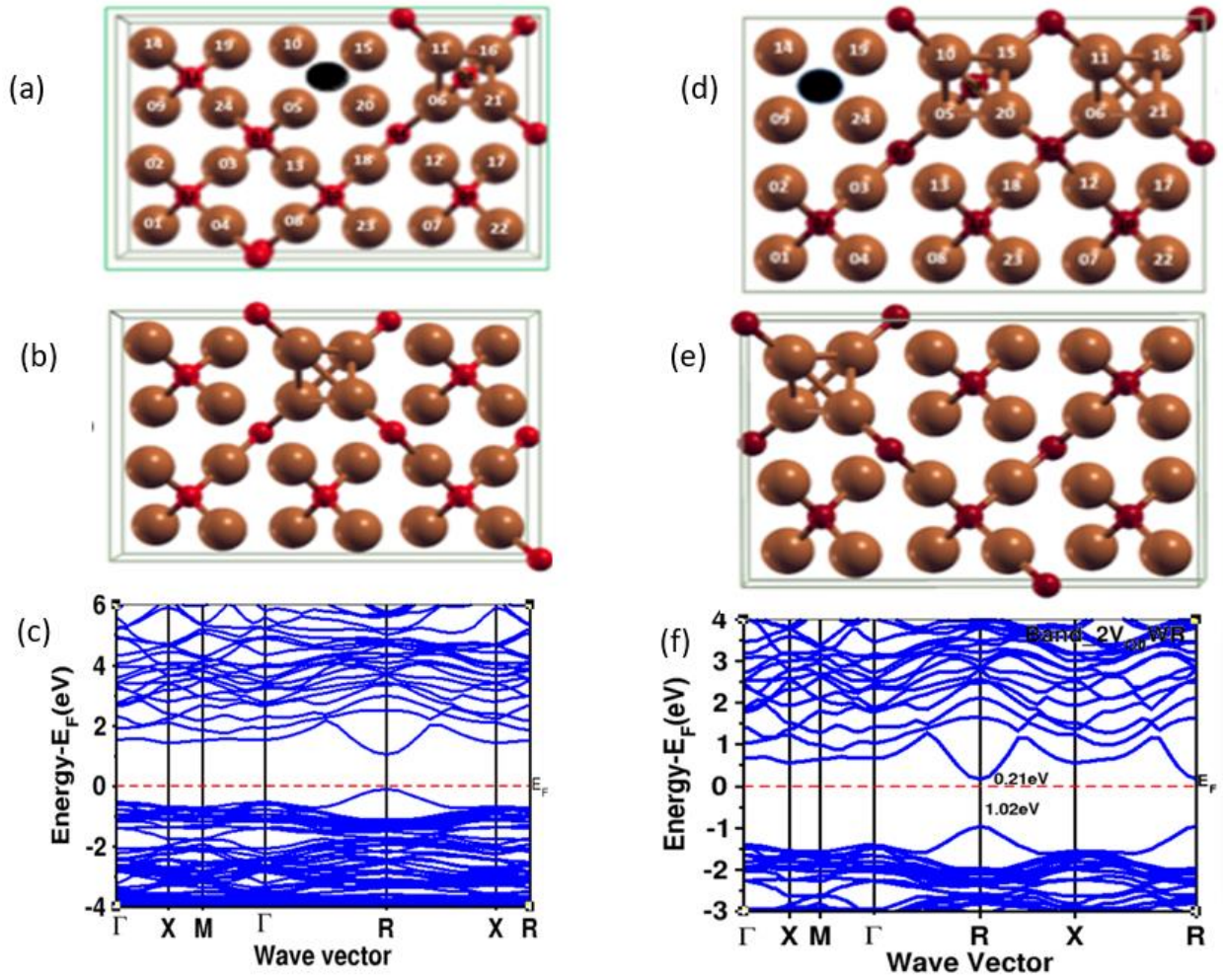

Figure 6. Structure (a,b, and c) represent oxygen replacement and vacancy point before relaxation, and after relaxation with band structure for Cu_2O. While (d,e and f) represent second oxygen replacement and vacancy point before and after relaxation with band structure The brown, and red spheres represents Cu and O atom respectively while the black sphere represent the vacant sites.

After first vacancy replacement, the atomic arrangement likely indicates some disturbance due to the replacement, which would lead to local distortions around the vacancy site. The system after been relaxed, allow the atoms to find a more stable configuration. Relaxation usually reduces internal stresses, leading to slight shifts in atomic positions. These shifts aim to minimize the system's energy, thereby stabilizing the structure after the vacancy replacement. The band structure indicates how the electronic properties have changed after the first oxygen vacancy was replaced. Defect states might have formed, altering the electronic band gap. These states can be seen as additional energy levels within the gap or modifications of the conduction/valence bands.

The shift in the Fermi level or the appearance of new states induces more conductivity or other electronic properties.

After second vacancy replacement, the distortion and changes in the atomic structure is more pronounced, as the local environment around each vacancy site is altered. Similar to the first case, relaxation helps the structure reach a more stable state after the second replacement. The atomic positions will adjust further, potentially leading to larger shifts compared to the single vacancy case, as the structure compensates for both vacancies. The band structure now reflects

the influence of two oxygen vacancies, introducing more defect states, further modifying the band gap and the overall electronic properties which shows additional states within the gap, reduced bandgap energy, with significant changes depending on how the vacancies interact with the material's electronic structure.

Replacing oxygen atoms with vacancies or other species introduces significant local distortions, which are partially alleviated by relaxation. This process allows the material to reach a lower-energy configuration, albeit one that is still perturbed compared to the perfect lattice. This significantly affects the electronic structure. The band structures (Figure 6c) and (Figure 6f) show that the replacement of oxygen atoms introduces defect states within the band gap. As more vacancies are introduced, these states become more prominent, and the overall electronic properties of Cu_2O are altered. This can lead to changes in conductivity, potentially increasing n-type behavior or even leading to metallic states if enough vacancies are introduced.

We observed that the Fermi level shift, which indicates that the replacement of oxygen atoms also shifts the Fermi level closer to the conduction band or mid-gap states, indicating a change in the material's electronic balance, possibly enhancing its conductivity or altering its semiconducting nature.

Table 5: Showing the calculated bond angles of first and second oxygen vacancy WR

Type of Calculations	Before Relaxation		After Relaxation	
	Atomic ID of Angle	Angle (^{0})	Atomic ID of Angle	Angle (^{0})
$1V_{OI}$	Cu06∠O29∠Cu21	112.576	Cu06∠O27∠Cu21	111.182
	Cu06∠O29∠Cu11	117.529	Cu06∠O27∠Cu11	106.429
	Cu16∠O29∠Cu21	117.529	Cu16∠O27∠Cu21	109.615
	Cu16∠O29∠Cu11	112.576	Cu16∠O27∠Cu11	111.182
$2V_{OII}$	Cu24∠O32∠Cu14	111.209	Cu24∠O30∠Cu14	111.205
	Cu24∠O32∠Cu19	109.285	Cu24∠O30∠Cu19	106.494
	Cu14∠O32∠Cu09	106.465	Cu14∠O30∠Cu09	108.936
	Cu09∠O32∠Cu12	111.209	Cu09∠O30∠Cu12	111.205

The distortion effect and the structural adjustment of the system WR and WOR caused by the removal and replacement of oxygen atom indicates that the system possessing electronic degeneracy will be unstable and will undergo distortion to form a system of lower symmetry as well as lower energy in order to remove the degeneracy. This effect is termed Jahn Teller distortion effect and it either elongates or compresses the bonds which reflect on the electronic structure of the system. The effect of the oxygen vacancy and its replacement affects the Cu-O, Cu-Cu bond length hereby causing an oxygen displacement and making the orbital overlaps with the Cu-d, O-p, Cu-p, O-s and Cu-s orbitals of the host lattice to modify the conduction band edge. The removal of O atom does not induce large distortion in the Cu_2O cell, except for the oxygen displacement generated by the Cu-O bond with different bond length of 1.8492 Å which is larger compared with the usual bond of 1.8412Å (Korzhavyi & Johansson, 2011). Table 6, below shows the measured bond length, for the first and second oxygen vacancy WR calculations while table 5 shows the bond angles as it affects the system

before and after relaxation. The bond length and angles are measured using xcrysden package.

Table 6: Showing the calculated bond length and formation energy of One and Two Oxygen Vacancy with Replacement

TYPE OF CALCULATIONS	BEFORE RELAXATION				AFTER RELAXATION				Band gap (eV)	FORMATION ENERGY (eV)
	ATOMIC ID	Cu-Cu (A^0)	Cu-O (A^0)	O-O (A^0)	ATOMIC ID	Cu-Cu (A^0)	Cu-O (A^0)	O-O (A^0)		
$1V_{OI}$	Cu6-Cu11	3.0198			Cu6-Cu11	2.9928			0.3	-6.669424267
	Cu15-O33		1.8492		Cu6-Cu16	3.0465				
	O27-O33			3.6985	Cu11-Cu21	3.0465				
					Cu16-Cu21	3.0446				
					Cu11-Cu16	3.0816				
					Cu6-Cu21	3.0816				
$2V_{OII}$					Cu6-Cu11	3.0360			0.66	0.680434612
					Cu6-Cu16	3.0492				
					Cu11-Cu21	3.0492				
					Cu16-Cu21	2.9933				
					Cu11-Cu16	3.0806				
					Cu6-Cu21	3.0806				
					Cu6-O29		1.8680			
					Cu11-O29		1.8680			
					Cu16-O29		1.8666			
					Cu21-O29		1.8666			
					O29-O41			3.7323		

CONCLUSION

In this paper we have analyzed the effect of oxygen vacancies on a 3x2x1 Cu_2O host. A single oxygen vacancy without doping exhibits both direct and indirect bandgap with a shift in the states was observed when compared with the pristine Cu_2O. We observed that when two oxygen vacancies are removed from the host Cu_2O there exist some Cu_3d states mix with the O 2s and over lapping Cu_4s valence band, leading to an increase of the width of the valence band as well as rises with more electronic states with a double state of about 0.13 eV and 0.81 eV for the valence band maximum, while conduction band bottom was showing predominantly the Cu_4s states with varied energy level. This suggest that the modulation defect that exist between the native point defect and the host cell shows a lower energy when the vacancy formation is odd and a higher energy state when it's even. The findings suggest that oxygen vacancies, particularly when not replaced, induce significant structural distortions that impact the material's electronic properties. These results pave the way for further investigations into potential dopants that could stabilize or enhance the optoelectronic properties of Cu_2O, offering promising avenues for material optimization in various applications. Thus, defect engineering via oxygen vacancy can modulate Cu_2O in such a way that the n-types semiconductor nature is revealed. However, the bandgaps obtain using the multiple vacancy are generally low compared with the one vacancy of up to 1.97eV.

Acknowledgments: The author expresses their gratitude to Tertiary Education Trust Fund (TET fund) in Abuja, Nigeria, and the Academic Staff Union of Universities (ASUU).

REFERENCES

Bogenrieder, S. E., Beßner, J., Engstfeld, A. K., & Jacob, T. J. T. J. o. P. C. C. (2024). First-Principles Study on the Structural and Magnetic Properties of Low-Index Cu2O and CuO Surfaces.

Cadi-Essadek, A., Roldan, A., Santos-Carballal, D., Ngoepe, P. E., Claeys, M., & de Leeuw, N. H. (2021). DFT+ U study of the electronic, magnetic and mechanical properties of Co, CoO, and Co3O4. *South African Journal of Chemistry*, *74*(1), 8–16-18–16.

Dongfang, N., Al-Hamdani, Y. S., & Iannuzzi, M. J. E. S. (2023). Understanding the role of oxygen-vacancy defects in Cu2O (111) from first-principle calculations. *5*(3), 035001.

Giannozzi, P., Baroni, S., Bonini, N., Calandra, M., Car, R., Cavazzoni, C.,…Dabo, I. (2009). QUANTUM ESPRESSO: a modular and open-source software project for quantum simulations of materials. *Journal of physics: Condensed matter*, *21*(39), 395502.

Hu, C.-C., Nian, J.-N., Teng, H. J. S. e. m., & cells, s. (2008). Electrodeposited p-type Cu2O as photocatalyst for H2 evolution from water reduction in the presence of WO3. *92*(9), 1071-1076.

Kirchner-Hall, N. E., Zhao, W., Xiong, Y., Timrov, I., & Dabo, I. (2021). Extensive benchmarking of DFT+ U calculations for predicting band gaps. *Applied Sciences*, *11*(5), 2395.

Korzhavyi, P. A., & Johansson, B. (2011). Literature review on the properties of cuprous oxide Cu {sub 2} O and the process of copper oxidation.

Li, L., Cheng, Y., Wang, W., Ren, S., Yang, Y., Luo, X., & Liu, H. (2011). Effects of copper and oxygen vacancies on the ferromagnetism of Mn-and Co-doped Cu2O. *Solid state communications*, *151*(21), 1583-1587.

Li, L., Zhang, R., Vinson, J., Shirley, E. L., Greeley, J. P., Guest, J. R., & Chan, M. K. J. C. o. M. (2018). Imaging catalytic activation of CO2 on Cu2O (110): a first-principles study. *30*(6), 1912-1923.

Perdew, J. P., Burke, K., & Ernzerhof, M. J. P. r. l. (1996). Generalized gradient approximation made simple. *77*(18), 3865.

Tarantino, S. C., Giannini, M., Carpenter, M. A., & Zema, M. J. I. (2016). Cooperative Jahn–Teller effect and the role of strain in the tetragonal-to-cubic phase transition in MgxCu1− xCr2O4. *3*(5), 354-366.

Visibile, A., Wang, R. B., Vertova, A., Rondinini, S., Minguzzi, A., Ahlberg, E., & Busch, M. J. C. o. M. (2019). Influence of strain on the band gap of Cu2O. *31*(13), 4787-4792.

Wang, Y., Wisesa, P., Balasubramanian, A., Dwaraknath, S., & Mueller, T. J. C. M. S. (2021). Rapid generation of optimal generalized Monkhorst-Pack grids. *187*, 110100.

Zhuang, G., Chen, Y., Zhuang, Z., Yu, Y., & Yu, J. J. S. C. M. (2020). Oxygen vacancies in metal oxides: recent progress towards advanced catalyst design. *63*(11), 2089-2118.